Silicon nanowires

DOI: 10.1002/smll.200800588

In Situ Laser Synthesis of Si Nanowires in the Dynamic TEM**

Mitra L. Taheri, Bryan W. Reed, Thomas B. LaGrange, and Nigel D. Browning*

Nanowires (NWs) are a crucial component in today's nanoscale devices and are vital to the further development of nanotechnology. To achieve reliable growth of NWs and uniform electronic properties, the specific mechanisms that control the structural development of NWs and the correlation between NWs and their nucleation and growth processes must be examined. Because imaging is not possible in Chemical Vapor Deposition (CVD) chambers, in situ transmission electron microscope (TEM) based growth methods provide a method for characterizing NW evolution. In this paper, we describe a new method of in situ synthesis and imaging of NWs using laser-assisted growth inside a TEM.

The vapor-liquid solid (VLS) growth mechanism (Figure 1), first described by Wagner and co-workers,[1,2] is a widely accepted description of how many 1D nanostructures are formed. VLS and similar models have been applied to such methods as hybrid pulsed-laser ablation/chemical vapor deposition (PLA/CVD)[9] and laser assisted NW growth at elevated temperatures,[10–14] in which a pulsed laser ablates a target with gas flowing through the reaction chamber held at elevated temperature. These methods have successfully produced semiconductor and conducting oxide[3] NWs with size control determined by the catalyst droplet diameter.[4] The VLS description of NW growth is a widely accepted model, but the exact role of vapor species and its interaction with the catalyst particle is not fully understood. For example, NW growth has been observed to occur far below predicted eutectic temperatures,[5,6] which suggests that alternative mechanisms such as solid-liquid-solid growth (SLS) may play a role.[7,8] Many NW fabrication techniques preclude direct in situ characterization of the growth process. Because of this need for direct observation during growth, TEM-based NW growth methods have become increasingly popular.[15–17] Though progress has been made in the study of the VLS mechanism of NW growth using in situ TEM, conventional in situ growth experiments are limited by the standard video frame rate (~30 Hz). Due to this limitation, relationships between reactant incorporation and transport, catalyst-wire interface development, and wire growth texture remain somewhat unclear. Moreover, laser-assisted phenomena (PLA or PLA/CVD) cannot be studied with conventional in situ TEM, which is typically performed with environmental TEM techniques using resistive heating.[15–17] A novel form of in situ TEM for the study of NW growth by laser-assisted techniques is described in this paper.

Here we present an in situ method for PLA synthesis of 1D nanostructures using the dynamic transmission electron microscope (DTEM)[18,19] that will permit the details of laser-assisted NW synthesis to be elucidated. The DTEM, schematically shown in Figure 2, consists of a TEM column (JEOL 2000FX) to which a pulsed Nd:YAG laser, labeled "hydro-drive laser" in Fig. 2, is added. This laser is incident directly on the sample and can be operated at 1064, 532 or 355 nm. The direct delivery of energy initiates a phase change or reaction that is investigated in situ during the experiment. Thus, the microscope can be used to fabricate NWs while simultaneously characterizing the reaction products created by each laser pulse. A second pulsed laser (15-ns-duration frequency-quintupled Nd:YLF) added to the column (labeled "cathode laser" in Figure 2) enables operation in both a pulsed photoemission and conventional thermionic continuous-wave (CW) electron beam imaging modes.[19] The pulsed mode's nanosecond-scale imaging capability greatly exceeds the ~30 Hz time resolution of conventional in situ TEM and can potentially provide a detailed understanding of NW growth. Time-resolved imaging experiments aimed at capturing the intermediate states at nanosecond time scales in PLA NW growth are underway and will be addressed in a future publication. In this paper, we present results obtained using in situ imaging in conventional CW imaging mode, but taking advantage of the DTEM's in situ laser drive capability. Specifically, we will present the first results using the sample ("hydro-drive") laser at 355 nm to stimulate the growth of the nanostructures, therefore revealing the DTEM as a tool for in

[*] Drs. M. L. Taheri,[#] B. W. Reed, T. B. LaGrange, N. D. Browning
Lawrence Livermore National Laboratory
Chemistry, Materials, Earth & Life Sciences
7000 East Avenue
Livermore, CA 94550

[#]Current Contact Information: Department of Materials Science & Engineering, Drexel University, Philadelphia, PA, USA
E-mail: mtaheri@coe.drexel.edu

[**] This work performed under the auspices of the U.S. Department of Energy by Lawrence Livermore National Laboratory and supported by the Office of Science, Office of Basic Energy Sciences, Division of Materials Sciences and Engineering, of the U.S. Department of Energy under Contract DE-AC52-07NA27344. The authors acknowledge support of the National Center for Electron Microscopy, Lawrence Berkeley Lab, which is supported by the U.S. Department of Energy under Contract # DE-AC02-05CH11231. The authors thank Blake Simpkins of the Naval Research Laboratory for providing the Si/Au samples, Rick Gross for assistance in sample preparation, and Richard Shuttlesworth and Benjamin Pyke for technical support on the Dynamic TEM. M.T. thanks Alfredo Morales of Sandia National Laboratory and Peidong Yang of UC Berkeley for useful discussions with respect to nanowire growth.

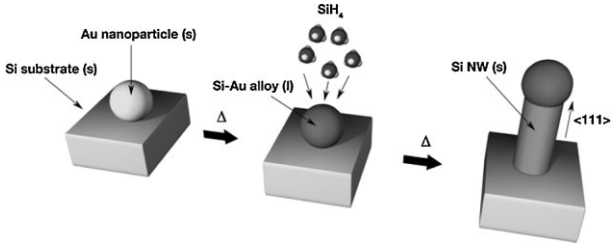

Figure 1. Schematic drawing of the Vapor-Liquid-Solid method of NW growth, after Wagner.[1,2]

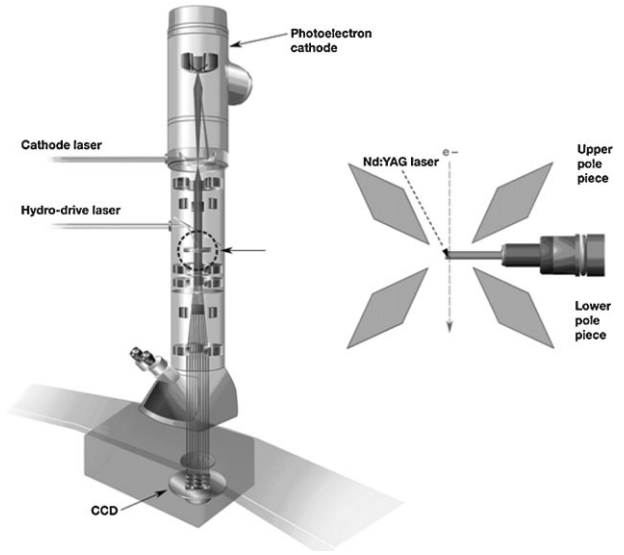

Figure 2. Schematic diagram of the DTEM apparatus (modified JEOL 2000FX TEM). The drive-laser configuration is blown up on the right. A schematic of the sample region (holder in pole piece gap) shows that the beam path comes in at a 40° angle to the sample surface; this laser treats (heating or ablation) the sample. The electron beam is normal to the sample surface, and electrons pass through the sample for imaging (labeled "e-").

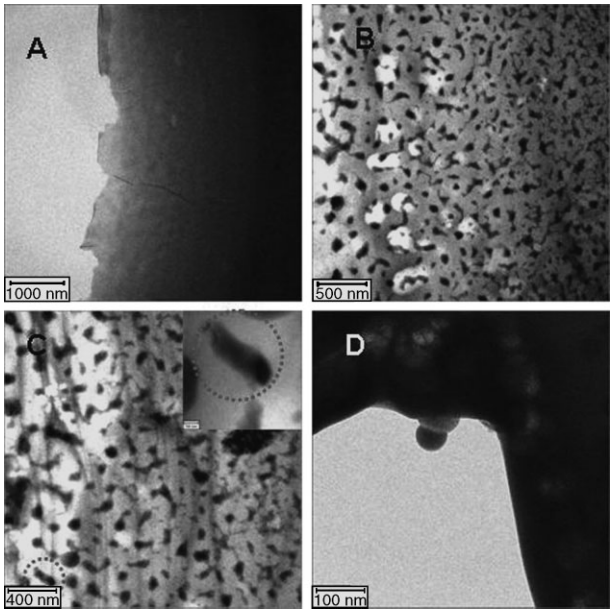

Figure 3. Images of the initial stages of Si NW development during laser heating. A. Crystalline Si <111> sample with 4 nm Au layer, before laser treatment. B. After 10 laser pulses (8 ns each) below the ablation threshold. C. After 10 additional laser pulse (20 total pulses) below the ablation threshold. D. Image of a wire with a distinct catalyst bulb at the edge of the sample.

situ imaging of nanostructure synthesis (see the experimental section for details of the NW synthesis procedure).

Wires produced in the DTEM were similar to those produced using *ex situ* laser assisted growth experiments,[9–14] yet did not require gas flow or resistive heating. The NW production was monitored in situ during pulsing using CW electron beam imaging in the DTEM. Figures 3 and 4 depict images collected during the growth of a Si NW by laser-heating and laser ablation, respectively. The images in Figure 3 were taken in situ in the DTEM during pulsed heating of the sample using CW imaging in the DTEM. Laser heating is shown to develop early stages of NW growth: balling up of the Au film, alloying, and initial wire growth. The sample was treated with 10 drive laser pulses between the first and second images and 10 additional drive laser pulses between images B and C. We found that heating was capable of producing some of the initial catalyst alloying steps in the VLS process, however the wire growth appears to have been halted regardless of further laser pulses at these energy levels (below the ablation threshold), thus the VLS process could not continue.

Because conventional VLS experiments (e.g., CVD) require a vapor species (e.g., SiH_4) to adsorb on the catalyst surface during growth, we also treated the sample above the ablation threshold to produce vapor. Unlike the heating experiments which only produced the initial stages of NW growth, these PLA experiments yielded crystalline wires up to and more than 1 μm in length appearing near the edges of the ablated regions, in areas that were heated but not ablated during the laser pulse (Figure 4). These regions experienced a brief but intense flux of silicon atoms during the pulse. The presence of this vapor appears to be the crucial difference between the barely-nascent NWs shown in Figure 3 and

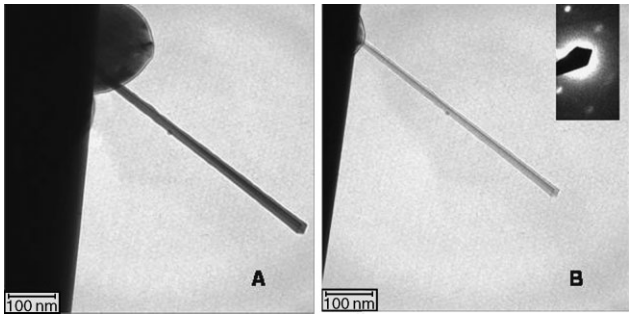

Figure 4. (a) Image of NW-like growth produced during PLA. b) Image of the same Si NW taken after laser ablation in the DTEM at different tilt angle; SAED pattern indicates crystallinity of the NW.

the well-developed crystalline NWs in Figure 4. The images in Figure 4 were taken in situ in the DTEM using CW imaging, during the ablation experiments.

It was evident that though the laser allowed controlled pulsed heating for initiating the growth of NWs, the PLA method was more successful in growing crystalline NWs with lengths comparable to those grown with the VLS method. To further examine the structure and morphology of the NWs grown by PLA, the NWs were characterized post-synthesis in an FEI Tecnai 200 kV TEM; these images are shown in Figure 5. Though none of the NWs shown in Figure 5 contain catalyst bulbs, we found that the 4 nm Au catalyst film layer played a crucial role in NW development: we carried out the same experiments on Si (111) films without an Au layer, and we could not grow NWs. Additionally, the difference between the stunted wires in Figure 3 and the well-developed wires in Figure 4 appeared to be related to the presence of silicon vapor

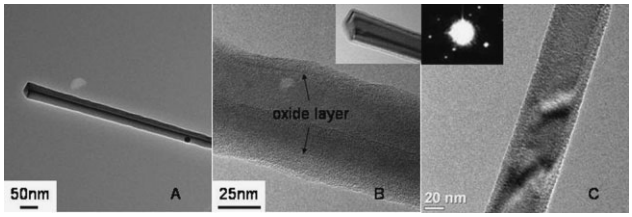

Figure 5. a) Bright-field (BF) TEM image of the wire shown in Figure 4. b) Higher-resolution image of the Si NW showing oxide shell; inset shows a larger image wire edge. c) BF TEM image of a different Si NW grown in the same batch, defocused to show Si core with oxide coating; SAED pattern indicates wire crystallinity.

in the latter case. To elucidate this further, we performed a calculation to estimate the reactant atom flux during PLA. These calculations show that there was a large enough flux to mimic some aspects of the VLS process, such as reactant adsorption on a wire or catalyst surface. The Si flux at the wire growth position was estimated from the volume of ablated material and the distance from the laser spot center. A single laser pulse creates a hole ~50 μm in diameter in the Si layer, with an average thickness of 100 nm. This volume contains $\sim 10^{13}$ Si atoms. We assume that these atoms disperse isotropically at ~1000 m/s $(\sim(kT/m)^{1/2}$ for Si at its normal boiling point), redepositing on the first surface they encounter. Thus, a growth site ~5 μm from the edge of the ablated region is bombarded with some 900 Si atoms/nm^2 within ~100 nanoseconds after the pulse; this greatly exceeds the flux density of residual gas molecules ($\sim 10^{-6}$ torr). The flux density is equivalent to an 18 nm solid thickness, yet the wires grew to more than 1 μm in length. Therefore, the direct Si flux to the surface of the growing wire does not account for all of the material. This suggests that most of the Si arrives through an indirect path, such as by first dissolving in the Au catalyst before diffusing to the NW growth site. Molecular dynamics of the PLA process, coupled with time-resolved imaging in the DTEM, are underway to understand the behavior of the Si atoms at the redeposition site leading to NW nucleation and growth.[20]

To clarify our calculations and to propose a growth mechanism, we analyzed samples ex situ from the initial stages of growth using Z-contrast imaging and Energy Dispersive Spectroscopy (EDS) in a JEOL 2500SE TEM. In Figure 7 the stages are labeled "1" and "2", and correspond to the steps outlined in Figure 6. The image labeled "3" is repeated from Figure 4. The long crystalline NW (image "4") is the final stage. EDS revealed that the initial pulsing produces Au "balling up", followed by alloying of Au and Si to form a catalyst. Unlike classical VLS growth, this PLA synthesis method produced NWs lacking catalyst bulbs at their free ends. Thus, with the calculations of atom flux during PLA and the observed structure and morphology of the NWs, we propose the following mechanism for NW growth via PLA: the 4 nm Au film is broken up into Au droplets and/or particles with the initial laser pulse. Further pulses form an alloy of SiAu, which acts as a catalyst. Thereafter, additional pulses allow the ablated 100–1000 Si atoms/nm^2 to redeposit onto the remaining Si substrate and SiAu catalysts, providing a sudden, intense influx of heat and of fast-moving, non-equilibrated

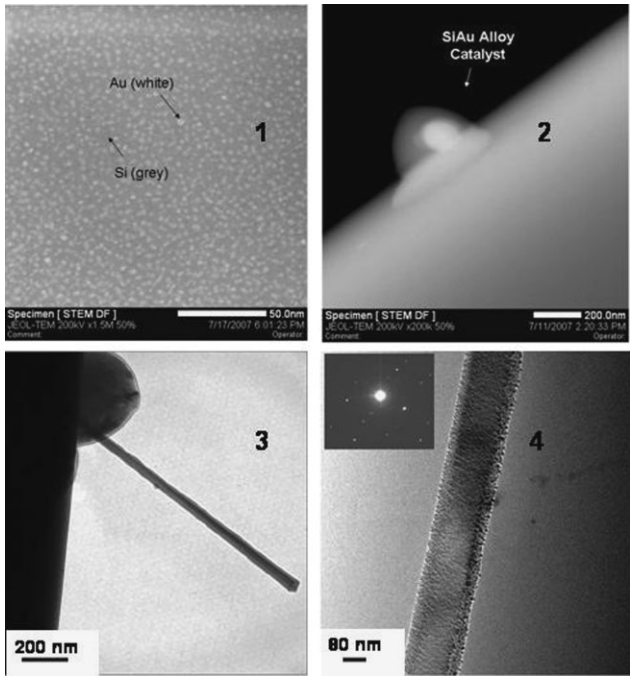

Figure 6. 1) STEM image of an Si <111> film with 4-nm Au shot, after a 355-nm Nd:YAG laser pulse at 240 μJ. Laser broke up the Au film into spheres. 2) STEM image from a sample after >1 pulse, indicating alloying of Si and Au to form a SiAu catalyst. 3) BF TEM image taken in the DTEM shows root-based growth of a Si NW out of the SiAu alloy catalyst. 4) BF TEM image of a Si NW grown using PLA in the DTEM (SAED pattern indicates crystallinity of the wire).

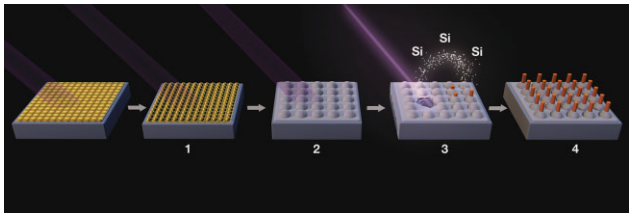

Figure 7. Proposed growth mechanism of Si NWs during PLA in the DTEM. 1) "Balling up" of 4-nm layer of Au. 2) Alloying of Si and Au to form a catalyst site. 3) Initial growth of Si NW from SiAu catalyst site. 4) Continued growth of NW.

silicon atoms. As the system relaxes toward thermal equilibrium and gradually cools, excess Si atoms find their way onto the fast-growing (111) face on the end of the emerging Si NW, resulting in the catalyst-wire morphology shown earlier in Figures 5b and 5c. This mechanism is shown in Figure 7.

In summary, we present a demonstration of the DTEM as a tool in which NWs may be imaged during PLA synthesis. Thus, in future we will be able to determine the local microstructure and morphology before, during and after laser-assisted NW formation, giving us insight into the processing parameters that influence growth. Si NWs were fabricated without resistive heating or the flow of reactant gases. This work establishes the ability to fabricate nanoscale systems in the DTEM under non-equilibrium conditions while simultaneously having the ability to image the growing nanostructures after each laser pulse. The initial results presented in this letter

focus on the controlled synthesis capabilities of the hydro-drive laser in the DTEM, and suggest that the DTEM may allow the complexity of the VLS mechanism to be evaluated without the need of external gas delivery (i.e. SiH_4) to the growth substrate. This capability opens the door to the development of routine nanoscale engineering methods (as opposed to the trial and error methods currently employed). A complete understanding of the origin of texture, morphology and extended defects in NWs during nucleation and growth will allow for a more comprehensive model of the mechanisms involved in 1D nanostructure production, and hence have a great impact on the future of the use of NWs in electronic device fabrication.

Experimental Section

Experimental Apparatus and Laser Parameters for NW Synthesis: DTEM experiments were carried out in a modified JEOL 2000FX TEM by hitting a sample with the hydro-drive laser (at a 43° angle and 355 nm wavelength) and viewing the synthesis reaction in situ using electron beam imaging (Figure 2). The images were collected using a standard single-electron-sensitive TVIPS camera. The laser energy can be adjusted for heating, melting or ablation. Its energy distribution is Gaussian, within a 2000 μm^2 spot size. The ablation thresholds reported by Gusev and co-workers[21,22] for 355 nm laser treatments of Si were used as guidelines. Films of <111> Si with a 4 nm Au layer (as a catalyst) were treated with a frequency tripled (355 nm) Nd:YAG laser with 8 ns pulses at 200–275 μJ (for heating or ablation). The ablation threshold for the Si/Au samples was observed to be 240 μJ (larger than quoted levels for ablation in the literature, possibly due to the Au layer reflecting the beam). Treatments at energies below the ablation threshold were considered "heating", while treatments above are referred to as "ablation". Gas was not introduced into the TEM chamber. NWs were produced by varying only one parameter: laser intensity.

Keywords:
TEM · nanowires · lasers · ablation

[1] R. S. Wagner, W.C Ellis,, *Appl. Phys. Lett.* **1964**, *4*, 89–90.
[2] R. S. Wagner, W. C. Ellis, K. A. Jackson, S. M. Arnold, *J. Appl. Phys.* **1964**, *35*, 2993–3000.
[3] M. Law, J. Goldberger, P. Yang, *Annu. Rev. Mater. Res.* **2004**, *34*, 83–122.
[4] Y. Wu, L. Huynh, C. J. Barrelet, D. C. Bell, C. M. Lieber, *Nano Lett.* **2004**, *4*, 433–436.
[5] T. I. Kamins, R. Stanley Williams, Y. Chen, Y.-L. Chang, Y. A. Chang, *Appl. Phys. Lett.* **2000**, *76*, 562–564.
[6] A. I. Persson, M. W. Larsson, S. Stenstron, B. J. Ohlsson, L. Samuelson, L. R. Wallenberg, *Nature Materials* **2004**, *3*, 677–681.
[7] T. Trentler, K. H. Hickman, S. C. Goel, A. M. Viano, P. C. Gibbons, W. E. Buhro, *Science* **1995**, *270*, 1791–1794.
[8] H. Yu, W. E. Buhro, *Adv.Mater.* **2003**, *15*, 416–419.
[9] Y. Wu, R. Fan, P. Yang, *Nano Lett.* **2002**, *2*, 83–86.
[10] A. M. Morales, C. M. Lieber, *Science* **1998**, *279*, 208–211.
[11] X. Duan, C. M. Lieber, *J. Am. Chem. Soc.* **2000**, *122*, 188–189.
[12] N. Wang, Y. H. Tang, Y. F. Zhang, C. S. Lee, S. T. Lee, *Phys. Rev. B* **1998**, *58*, R16024–R16026.
[13] K. Wang, S. Y. Chung, D. Kim, *Appl. Phys. A* **2004**, *79*, 895–897.
[14] J. J. Gole, J. D. Stout, W. L. Rauch, Z. L. Wang, *Appl. Phys. Lett.* **2000**, *76*, 2346–2348.
[15] S. Kodambaka, J. B. Hannon, R. M. Tromp, F. M. Ross, *Nano Lett.* **2006**, *6*, 1292–1296.
[16] E. A. Stach, P. J. Pauzauskie, T. Kuykendall, J. Goldberger, R. He, P. Yang, *Nano Lett.* **2003**, *3*, 867–869.
[17] Y. Wu, P. Yang, *J. Am. Chem. Soc.* **2001**, *123*, 3165–3166.
[18] T. Lagrange, M. R. Armstrong, K. Boyden, C. G. Brown, G. H. Campbell, J. D. Colvin, W. J. Dehope, A. M. Frank, D. J. Gibson, F. V. Hartemann, J. S. Kim, W. E. King, B. J. Pyke, B. W. Reed, M. D. Shirk, R. M. Shuttlesworth, B. C. Stuart, B. R. Torralva, N. D. Browning, *Appl. Phys. Lett.* **2006**, *89*, 044105-1.
[19] W. E. King, M. Armstrong, V. Malka, B. W. Reed, A. Antoine Rousse, *MRS Bulletin*, **2006**, *31*, 614–619.
[20] M. Upmanyu, to be published (**2008**).
[21] A. Frass, A. Lomonosov, P. Hess, V. Gusev, *J. Appl. Phys.* **2000**, *87*, 3505–3510.
[22] V. Gusev, A. A. Kolomenskii, P. Hess, *Appl. Phys. A: Mater. Sci. & Proc.* **1995**, *61*, 285–298.

Received: April 24, 2008
Revised: July 29, 2008
Published online:

